

# Theory of Tunneling Spectroscopy in Superconducting Topological Insulator

Ai Yamakage,<sup>1</sup> Keiji Yada,<sup>1</sup> Masatoshi Sato,<sup>2</sup> and Yukio Tanaka<sup>1</sup>

<sup>1</sup>*Department of Applied Physics, Nagoya University, Nagoya 464-8603, Japan*

<sup>2</sup>*Institute for Solid State Physics, University of Tokyo, Chiba 277-8581, Japan*

(Dated: August 26, 2019)

We develop a theory of the tunneling spectroscopy for the superconducting topological insulator (STI)  $\text{Cu}_x\text{Bi}_2\text{Se}_3$ , where Andreev bound states can become Majorana fermions. We calculate tunneling conductance between normal metal /STI junctions for possible candidates of the pairing symmetries realized in  $\text{Cu}_x\text{Bi}_2\text{Se}_3$ . A close comparison between the theory and the recent point contact experimental results by Sasaki *et al.* [Phys. Rev. Lett. **107**, 217001 (2011)] enables us to identify that the experimentally observed zero bias conductance peak stems from the Majorana fermions and gives a strong evidence for a topological superconductivity in  $\text{Cu}_x\text{Bi}_2\text{Se}_3$ .

PACS numbers: 74.45.+c, 74.20.Rp, 73.20.At, 03.65.Vf

Topological superconductors (TSCs) are a new state of matters which are characterized by two basic properties [1–3]. The first is the bulk property. They have bulk gaps due to the formation of Cooper pairs and support non-zero topological numbers of the bulk wave functions. The other is the boundary property. From the bulk-boundary correspondence, there exist topologically protected gapless surface Andreev bound states (SABSs). In particular, the superconductivity infers that the gapless SABSs are their own antiparticles, thus Majorana fermions. The realization of Majorana fermions in condensed matter physics is of particular interest because of their novelty as well as the possible application for quantum computing [4]. While schemes to realize Majorana fermions by using the spin-orbit interaction and the Zeeman magnetic field are very attractive [5–21], their experimental preparations are still ongoing.

The recent discovered superconductor  $\text{Cu}_x\text{Bi}_2\text{Se}_3$  [22–25] is a prime candidate of the TSC because of its peculiar band structure and strong spin-orbit coupling [26]. The base material  $\text{Bi}_2\text{Se}_3$  is a topological insulator with a topologically protected gapless Dirac fermion on its surface. With intercalating Cu, however, the superconductivity appears. From the Fermi surface structure of the material, it was predicted that the superconducting topological insulator (STI)  $\text{Cu}_x\text{Bi}_2\text{Se}_3$  must be a TSC [26] if time-reversal invariant odd-parity superconductivity is realized [27, 28]. Possible SABSs specific to this material have been predicted [26, 29], and the surface spectral functions have been calculated [30]. Indeed, a recent point-contact spectroscopy experiment [31] has reported a pronounced zero-bias conductance peak (ZBCP) which signifies unconventional superconductivity. With careful analysis excluding other mechanisms, it has been concluded that the ZBCP is intrinsic, and is a manifestation of the gapless SABS [31]. Similar ZBCPs have been observed by other groups independently as well [32–34].

The purpose of this work is to present a theory of the tunneling conductance for the STI, and to establish the origin of the ZBCP theoretically. Up to this time,

the surface local density of states (SLDOS) for the STI have been calculated to study the ZBCP theoretically [31]. If the SABS has a flat band structure, which is realized in high- $T_c$  cuprate, the tunneling conductance is indeed expressed by the SLDOS [35, 36]. In the present case, however, the correspondence is not clear. For the STI, the SABS has a linear dispersion. In this case, the SLDOS does not always express the tunneling conductance in normal metal (N)/superconductor junction [37–40], and the resultant tunneling conductance strongly depends on the transmissivity at the interface. Thus, in order to pursue the origin of the ZBCP in the STI, one needs to calculate directly the tunneling conductance of the N/STI junction by solving the Bogoliubov-de Gennes (BdG) equation.

In this letter, considering momentum independent gap functions, we calculate the tunneling conductance between N/STI junctions for all possible pairing symmetries consistent with the point group of  $\text{Cu}_x\text{Bi}_2\text{Se}_3$ . Our results are summarized in the Table I. We find that among four possible pairing symmetries, only two show ZBCPs in the tunneling spectra. Both of them are TSCs, and support Majorana fermions as gapless SABSs. Our analysis strongly supports that the ZBCP observed in Ref.[31] is originated from Majorana fermions, and it gives a firm evidence of topological superconductivity in  $\text{Cu}_x\text{Bi}_2\text{Se}_3$ . We also find differences in the tunneling spectra between these two pairing symmetries and discuss how to distinguish them experimentally.

Let us start with the BdG Hamiltonian,

$$H(\mathbf{k}) = (H_0(\mathbf{k}) - \mu)\tau_z + \hat{\Delta}\tau_x. \quad (1)$$

Here  $H_0$  is the Hamiltonian of the parent topological insulator  $\text{Bi}_2\text{Se}_3$  given by

$$H_0(\mathbf{k}) = m(\mathbf{k})\sigma_x + v_z k_z \sigma_y + \sigma_z(k_x s_y - k_y s_x), \quad (2)$$

$$m(\mathbf{k}) = m_0 + m_1 k_z^2 + m_2 k^2, \quad (3)$$

where  $\sigma_z = \pm 1$  labels the two Se-Bi  $p_z$  orbitals of  $\text{Cu}_x\text{Bi}_2\text{Se}_3$ ,  $k$  is the momentum in  $xy$ -plane defined by

$\hat{\Delta}$	$\Delta_{1a}$	$\Delta_{1b}$	$\Delta_2$	$\Delta_3$	$\Delta_4$
	1	$\sigma_x$	$\sigma_y s_z$	$\sigma_z$	$(\sigma_y s_x, \sigma_y s_y)$
Parity	$A_{1g}$	$A_{1u}$	$A_{1u}$	$A_{2u}$	$E_u$
Gap	iso	aniso	aniso	planer	polar
	full	full	full	point node	point node
low trans.	U	U	DP	V	ZBP
int. trans.	U	U	ZBP	V	ZBP

TABLE I: Momentum-independent odd- and even-parity pairing potentials in  $D_{3d}$  point group. The energy gaps are isotropic (iso), anisotropic (aniso) full gaps, or have point nodes at  $k_i$ -axis ( $i = x, y, z$ ). In the cases of low and intermediate (int.) transmissivity, the line shapes of tunneling conductance shows U-shape gap, V-shape dip, double peak (DP), and zero bias peak (ZBP) (see Fig.3 and the corresponding discussions in the text).

$k^2 = k_x^2 + k_y^2$ ,  $s_\mu$ , and  $\tau_\mu$  the Pauli matrices in the spin and the Nambu spaces, respectively [26].  $\hat{\Delta}$  is a  $4 \times 4$  matrix which denotes a gap function. When the pairing interaction is short-range and attractive, the gap function is momentum-independent. There are four possible time-reversal invariant pairings consistent with the crystal symmetry of  $\text{Cu}_x\text{Bi}_2\text{Se}_3$  [26],  $\Delta_1 = \Delta (\equiv \Delta_{1a})$  or  $\Delta\sigma_x (\equiv \Delta_{1b})$ ,  $\Delta_2 = \Delta\sigma_y s_z$ ,  $\Delta_3 = \Delta\sigma_z$ ,  $\Delta_4 = \Delta\sigma_y s_x$  [41]. For some of the pairings above, the spin helicity is a good quantum number, which enables us to simplify the BdG Hamiltonian Eq.(1): The pairings  $\Delta_{1a}$ ,  $\Delta_{1b}$  and  $\Delta_3$  preserve the helicity  $h = k_x s_y - k_y s_x$ , thus by diagonalizing  $h$ , Eq.(1) is reduced to the  $4 \times 4$  matrix,

$$H_{i,s}(\mathbf{k}) = m(\mathbf{k})\sigma_x\tau_z + v_z k_z \sigma_y \tau_z + s k \sigma_z \tau_z + \Delta_i \tau_x, \quad (4)$$

where  $sk = \pm k$  is an eigenvalue of  $h$ , and  $i = 1a, 1b, 3$ . In addition, in the pairing  $\Delta_2$ , the ‘‘modified’’ helicity  $h' = h\tau_z$  is conserved, thus we have

$$H_{2,s'}(\mathbf{k}) = m(\mathbf{k})\sigma_x\tau_z + v_z k_z \sigma_y \tau_z + s' k \sigma_z + \Delta\sigma_y \tau_x, \quad (5)$$

with  $s' = \pm$ . On the other hand, no preserving helicity exists in  $\Delta_4$ . Hereafter, we set  $\Delta = 0.6$  meV and  $m_1 = 20.18$  eV $\text{\AA}^2$  or  $m_1 = 5.66$  eV $\text{\AA}^2$ . The other parameters are the same as those used in Ref.[31], as summarized in Table II.

We first summarize bulk properties of superconducting states with these pairings. By straightforward diagonalization of the BdG Hamiltonian Eq.(1) [or its reduced ones Eqs.(4) and (5)], the bulk energy spectra are derived as

$$E_i(\mathbf{k}) = \sqrt{\xi^2(\mathbf{k}) \pm \eta_i^2(\mathbf{k})}, \quad (i = 1a, 1b, 2, 3, 4). \quad (6)$$

Here  $\xi(\mathbf{k})$  is a common part for all the pairings,  $\xi^2(\mathbf{k}) = \mu^2 + m^2 + \Delta^2 + v_z^2 k_z^2 + v^2 k^2$ , and  $\eta_i(\mathbf{k})$ s' are pairing de-

$m_0$	$m_1$	$m_2$	$v_z$	$v$	$\mu$	$\Delta$
-0.28	20.18	56.6	3.09	4.1	0.5	0.6
(eV)	(eV $\text{\AA}^2$ )	(eV $\text{\AA}^2$ )	(eV $\text{\AA}$ )	(eV $\text{\AA}$ )	(eV)	(meV)

TABLE II: Material parameters for  $\text{Cu}_x\text{Bi}_2\text{Se}_3$ , taken from Ref. [31].

pendent parts given by

$$\begin{aligned} \eta_{1a}^2 &= 2\mu\sqrt{m^2 + v_z^2 k_z^2 + v^2 k^2}, \\ \eta_{1b}^2 &= 2\sqrt{\mu^2 m^2 + (v_z^2 k_z^2 + v^2 k^2)(\mu^2 + \Delta^2)}, \\ \eta_2^2 &= 2\sqrt{m^2(\Delta^2 + \mu^2) + \mu^2(v_z^2 k_z^2 + v^2 k^2)}, \\ \eta_{3,4}^2 &= 2\sqrt{\mu^2(m^2 + v_z^2 k_z^2 + v^2 k^2) + \Delta^2(m^2 + \zeta_{3,4}^2)}, \end{aligned} \quad (7)$$

with  $\zeta_3^2 = v_z^2 k_z^2$  and  $\zeta_4^2 = v^2 k_y^2$ . The polar plots of the energy gaps  $E_g$ , which are the minimum values of  $E_i(\mathbf{k})$  with a fixed angle of  $\mathbf{k}$ , are shown in Fig.1. While the energy dispersions  $E_{1a}$ ,  $E_{1b}$ ,  $E_2$  are full gapped,  $E_3$  and  $E_4$  have point nodes on the  $k_z$  axis and the  $k_y$  axis, respectively. Another important property is parity of the pairings. Because the parent material  $\text{Bi}_2\text{Se}_3$  preserves the parity  $P = \sigma_x$ , the pairing function must be a parity eigenstate. Among the possible pairings above, only  $\Delta_1$  is even-parity and others are odd-parity. From a general theory of topological odd-parity superconductors [27, 28] and its specific band structure, these odd-parity pairings imply the topological superconductivity of  $\text{Cu}_x\text{Bi}_2\text{Se}_3$ . In fact, they are characterized by the bulk nonzero topological number called ‘‘mod-2 winding number’’ even if they support point nodes in the gap functions [31].

Next, we solve SABS on the (111) surface normal to the  $z$ -axis. For each pairing, we consider a semi-infinite superconductor in  $z > 0$  with a flat surface at  $z = 0$ . The wave function is given by

$$\psi_{k_x, k_y, E}(z > 0) = \sum_I t_I u_I e^{iq_I z} e^{ik_x x} e^{ik_y y}, \quad (8)$$

where  $u_I$ s' are the eigenvectors of the BdG Hamiltonian Eq.(1) for up-going or dumping states with the

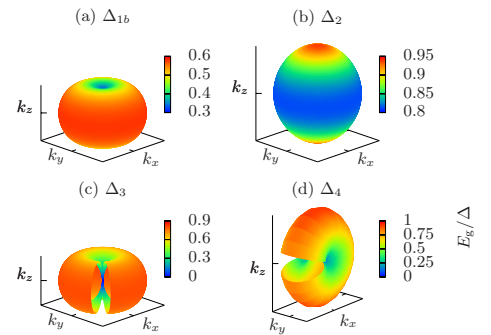


FIG. 1: Polar plots of the bulk superconducting gap  $E_g$  for  $\Delta_{1b}$ ,  $\Delta_2$ ,  $\Delta_3$ , and  $\Delta_4$ . It is not plotted in a certain region for the cases (d) and (e), for visibility.

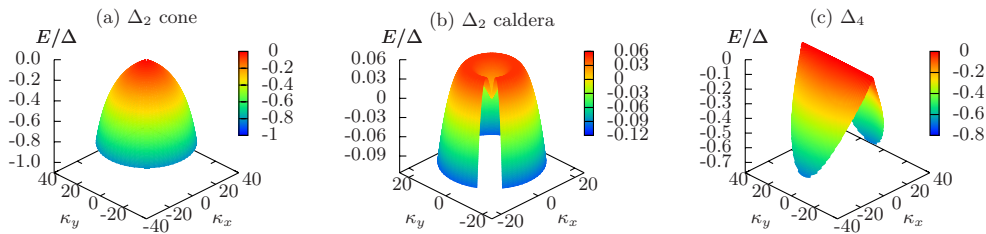


FIG. 2: Energy dispersion relations of the gapless SABSS. Here  $\kappa_i$  is the normalized momentum,  $\kappa_i = \sqrt{m_2}k_i/\sqrt{\Delta}$ . The energy dispersions are shown in the entire region for case (a) and (c), and only in the region of  $E > -0.1\Delta$  for case (b). The model parameters are the same as those in Table II except for  $m_1 = 5.66 \text{ eV}\text{\AA}^2$  in the case (b).

momentum  $\mathbf{k} = (k_x, k_y, q_I)$  and the energy  $E$ . Here  $q_I$  satisfies  $E_i(k_x, k_y, q_I) = E$  with  $E_i(\mathbf{k})$  in Eq.(6), and  $\partial E_i(k_x, k_y, q_I)/\partial q_I > 0$  for the up-going states, and  $\text{Im } q_I > 0$  for the dumping states, respectively. The coefficients  $t_{I\sigma}$  are determined by the boundary condition at  $z = 0$ , *i.e.*  $\psi_{k_x, k_y, E}(z = 0) = 0$ .

We find that there exist well-localized gapless SABSS in the cases with  $\Delta_2$  and  $\Delta_4$ . They satisfy the Majorana condition,  $\psi(z) = \psi^*(z)$ , thus they are Majorana fermions. For  $\Delta_2$ , two different SABSS are possible, as illustrated in Figs. 2(a) and (b). When  $m_1 = 20.18 \text{ eV}\text{\AA}^2$ , the energy spectrum of the SABSS is an axial symmetric monotonic function of  $k$ , and its shape is a simple cone [Fig. 2(a)]. On the other hand, when  $m_1 = 5.66 \text{ eV}\text{\AA}^2$ , a second crossing of the zero energy appears at finite  $k$  and a *caldera*-shaped cone is realized [Fig. 2(b)]. This result is consistent with that in Refs.[29, 30]. In the case with  $\Delta_4$  [Fig. 2(c)], the Majorana cone of the SABSS is deformed along the direction toward the point nodes in the bulk gap. The flat dispersion in this direction is a consequence of an accidental topological number existing in this case [42, 43]. We also notice that  $\Delta_3$  may support a gapless SABSS, but it is not well-separated from point node excitations on the (111) surface.

Now we calculate the tunneling conductance of N/STI junction, generalizing theories of the tunneling spectroscopy of conventional [44] and unconventional [45, 46] superconductors. We suppose a free electron in N with the Hamiltonian  $H_N(\mathbf{k}) = [(k_x^2 + k_y^2 + k_z^2)/(2m_e) - \mu_N]\sigma_0 s_0 \tau_z$ . The wave function in N ( $z < 0$ ) is given by

$$\psi_{k_x, k_y, E, \sigma, s}(z < 0) = \chi_{\sigma s e} e^{ik_x x + ik_y y + ik_e z} + \sum_{\sigma' s' \tau'} r_{\sigma s \sigma' s' \tau'} \chi_{\sigma' s' \tau'} e^{ik_x x + ik_y y - i\tau' k_\tau z}, \quad (9)$$

where  $\chi_{\sigma s \tau}$  is the eigenvector of  $H_N(\mathbf{k})$  with orbital  $\sigma$  and spin  $s$  for electron ( $\tau = +1$ ) or hole ( $\tau = -1$ ), and  $k_e = \sqrt{2m_e(\mu_N + E)}$  and  $k_h = \sqrt{2m_e(\mu_N - E)}$ . The first term of the wave function denotes an injected electron, and the second one denotes a reflected electron and hole with reflection coefficient  $r$ . On the other hand, the wave function in the STI side ( $z > 0$ ) is given by

Eq. (8) with the transmission coefficient  $t_I$ . These wave functions are connected at the interface ( $z = 0$ ) by the condition [47],

$$\psi(-0) = \psi(+0), \quad v(+0)\psi(+0) = v(-0)\psi(-0), \quad (10)$$

with the velocity operator,  $v(z) = \partial H / \partial k_z|_{k_z \rightarrow -i\partial_z}$ . Equation (10) determines the reflection and transmission coefficients  $r$  and  $t$ . Finally, the normalized charge conductance  $G$  is given by

$$\frac{G}{G_N} = \frac{\sum_{\sigma s} \int_0^{2\pi} d\phi \int_0^{\pi/2} d\theta \sin 2\theta T_{\sigma s}(\theta, \phi, eV)}{\sum_{\sigma s} \int_0^{2\pi} d\phi \int_0^{\pi/2} d\theta \sin 2\theta T_{\sigma s}(\theta, \phi, 0)|_{\Delta=0}}, \quad (11)$$

where  $T_{\sigma s}(\theta, \phi, E) = 4 - \sum_{\sigma' s' \tau'} \tau' |r_{\sigma s \sigma' s' \tau'}(k_x = k_e \sin \theta \cos \phi, k_y = k_e \sin \theta \sin \phi)|^2$  is the transmission probability, and the energy  $E$  of the injected electron is fixed at the bias voltage  $eV$ .

In the following, the band mass of N is fixed as  $m_e m_2 = 1$  for simplicity. We control the transmissivity of the N/STI interface by changing the value of  $\mu_N$ . For the material parameters in Table II, the highest transmissivity is accomplished when  $\mu_N/\mu \sim 0.6$  because the Fermi momentum in N coincides with that in STI. As  $\mu_N$  increases, lower transmissivity is realized.

The resulting tunneling conductances  $G/G_N$  as functions of bias voltage  $eV/\Delta$  are shown in Fig.3. In high transparent junctions ( $\mu_N/\mu = 0.6$ ), all the pairings show that  $G/G_N \sim 2$  for  $|eV/\Delta| < 1$  because the injected electron with  $E < |\Delta|$  is almost perfectly reflected as a hole due to Andreev reflection. On the other hand, in lower transparent junctions ( $\mu_N/\mu = 60, 1200$ ), the line shape of  $G$  strongly depends on the pairing symmetries: For  $\Delta_{1a}$  and  $\Delta_{1b}$ , we have *U*-shaped tunneling conductances similar to those of conventional *s*-wave superconductors [Figs.3(a) and (b)]. In comparison with conventional *s*-wave superconductors,  $\Delta_{1b}$  shows a broad coherence peak at  $eV = \pm\Delta$  in the low transparent limit ( $\mu_N/\mu = 1200$ ), but it is due to the anisotropy of the energy gap in the momentum space [Fig.1(a)]. We also have a *V*-shaped tunneling conductance for  $\Delta_3$  [Fig.3(e)], which is natu-

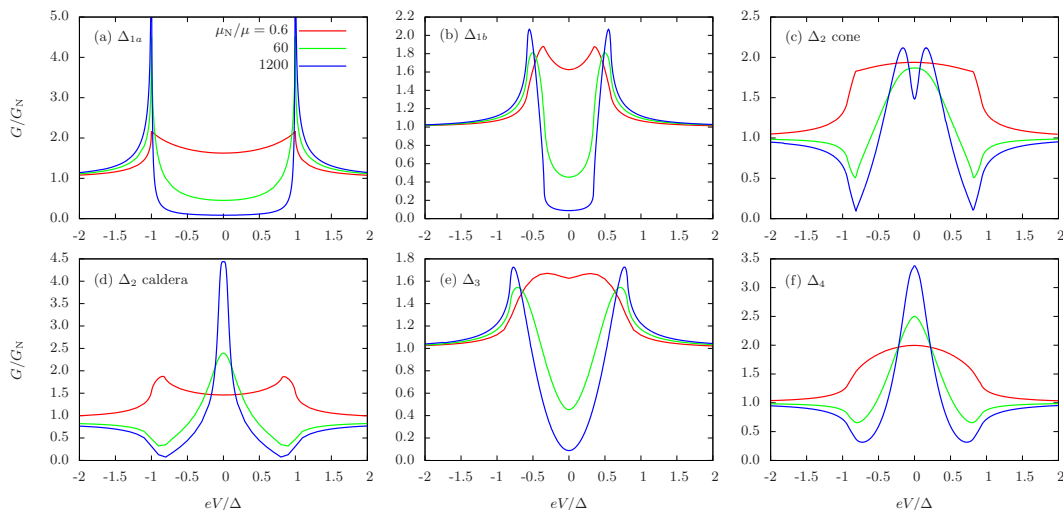


FIG. 3: The normalized tunneling conductances  $G/G_N$  as functions of bias voltage  $eV/\Delta$  for  $\Delta_{1a}$ ,  $\Delta_{1b}$ ,  $\Delta_2$ ,  $\Delta_3$ , and  $\Delta_4$ . The model parameters are the same as those in Table II except for  $m_1 = 5.66 \text{ eV\AA}^2$  in the case (d).

rally expected by the existence of point nodes located at the  $k_z$ -axis [Fig.1(c)].

For odd parity pairings  $\Delta_2$  and  $\Delta_4$  [Figs.3(c), (d) and (f)], we find that ZBCPs are generated in  $G/G_N$ , except for the low transparent limit  $\mu_N/\mu = 1200$  in Fig.3 (c). The ZBCPs stem from gapless SABSs illustrated in Fig.2. While  $G/G_N$  in Fig.3 (c) has a double-peak structure in the low transparent limit, it is consistent with the SLDOS of the SABS illustrated in Fig.2(a). (For the calculation of the SLDOS, see Supplemental Materials in Ref.[31].) We also find that the different behaviors between Fig.3(c) and Fig.3(d) can be understood from the difference in the SABSs. In both cases, the pairing symmetries are  $\Delta_2$ , but the shapes of the SABS are completely different. In the case of Fig.3(d) with  $m_1 = 5.66 \text{ eV\AA}^2$ , a *caldera-cone* is realized as the SABS, as shown in Fig.2(b). In this case, the energy of the SABS is zero not only at  $k = 0$  but also at finite  $k$ . Thus the SLDOS at zero energy is enhanced in comparison with that for  $m_1 = 20.18 \text{ eV\AA}^2$  where a conventional cone-shaped SABS is realized [Fig.2(a)]. As a result, even in low transparent limit  $\mu_N/\mu = 1200$ , no double-peak structure of  $G/G_N$  appears in Fig.3(d). In the case with  $\Delta_4$ , the SABS has a flat dispersion as mentioned before [Fig.2(c)]. The flat dispersion of the SABS gives a large SLDOS at zero energy, which makes a ZBCP in  $G/G_N$  for arbitrary lower transmissivity, as shown in Fig.3(f).

Finally, we compare our results with the experimentally observed tunneling spectroscopy in  $\text{Cu}_x\text{Bi}_2\text{Se}_3$ . The tunneling conductance in  $\text{Au/Ag/Cu}_{0.3}\text{Bi}_2\text{Se}_3$  junction has been observed in Ref.[31]. From the lattice constants of Au and Ag ( $a \sim 4\text{\AA}$ ) [48], the Fermi momentum of N is estimated as  $k_F \sim \pi/a \sim 1\text{\AA}^{-1}$ , which corresponds to  $\mu_N/\mu \sim 100$  in our model. While in the actual system, a barrier layer suppressing transmissivity could be

formed between N and STI, it can be taken into account as an effective increase of  $\mu_N/\mu$ . Therefore, the experiment result in Ref.[31] should be compared with ours with  $\mu_N/\mu > 100$ . From Fig.3, we find that the experimentally observed ZBCP is consistent only with  $\Delta_2$  and  $\Delta_4$ , both of which support ZBCPs originated from Majorana fermions on the N/STI interface.

Our results also suggest how to distinguish  $\Delta_2$  and  $\Delta_4$ . First of all, one can distinguish them by the specific heat. The analytic solutions of the quasiparticle spectra in Eq.(6) makes it possible to predict the detailed structure of the specific heat. In particular, the  $T^3$ -dependence of the specific heat expected for point nodes in  $\Delta_4$  can be predicted in details, which should be identified experimentally in homogeneous sample. We also notice that if the N/STI junction is prepared with much lower transmissivity, one may differentiate their tunneling conductances: Depending on parameters of system, a double peak structure appears in the tunneling conductance if the pairing symmetry is  $\Delta_2$ .

In conclusion, we have developed a theory of the tunneling spectroscopy for STI, and presented a full theoretical calculation of the tunneling spectra for all possible superconducting states of  $\text{Cu}_x\text{Bi}_2\text{Se}_3$ . A close comparison between the theory and the experiment enables us to identify that experimentally observed ZBCP by Sasaki *et al.* [31] is due to SABS hosting Majorana Fermions and gives a strong evidence for a topological superconductivity in  $\text{Cu}_x\text{Bi}_2\text{Se}_3$ . Our obtained results serve as a guide to explore novel topological superconductors with Majorana fermions [49].

We thank S. Kawabata, M. Kriener, K. Segawa, S. Sasaki and Y. Ando for useful discussions. MS thanks the Kavli Institute for Theoretical Physics, UCSB, for hospitality, where this research was completed. This work

was supported by MEXT (Innovative Area “Topological Quantum Phenomena” KAKENHI), and in part by the National Science Foundation under Grant No. NSF PHY05-51164.

- 
- [1] Y. Tanaka, M. Sato, and N. Nagaosa, *J. Phys. Soc. Jpn.* **81**, 011013 (2012).
- [2] X.-L. Qi and S.-C. Zhang, *Rev. Mod. Phys.* **83**, 1057 (2011).
- [3] A. P. Schnyder, S. Ryu, A. Furusaki, and A. W. W. Ludwig, *Phys. Rev. B* **78**, 195125 (2008).
- [4] F. Wilczek, *Nature Phys.* **5**, 614 (2009).
- [5] M.Sato and S.Fujimoto, *Phys. Rev. B* **79**, 094504 (2009).
- [6] M.Sato, Y. Takahashi, and S. Fujimoto, *Phys. Rev. Lett.* **103**, 020401 (2009).
- [7] M.Sato, Y. Takahashi, and S. Fujimoto, *Phys. Rev. B* **82**, 134521 (2010).
- [8] M. Sato and S. Fujimoto, *Phys. Rev. Lett.* **105**, 217001 (2010).
- [9] J.D.Sau, R.M.Lutchyn, S.Tewari, and S. D. Sarma, *Phys. Rev. Lett.* **104**, 040502 (2010).
- [10] J. Alicea, *Phys. Rev. B* **81**, 125318 (2010).
- [11] R. M. Lutchyn, J. D. Sau, and S. Das Sarma, *Phys. Rev. Lett.* **105**, 077001 (2010).
- [12] Y. Oreg, G. Refael, and F. von Oppen, *Phys. Rev. Lett.* **105**, 177002 (2010).
- [13] R. M. Lutchyn, T. Stanescu, and S. D. Sarma, *Phys. Rev. Lett.* **106**, 127001 (2011).
- [14] J. Alicea, Y. Oreg, G. Rafael, F. von Oppen, and M. F. Fisher, *Nat. Phys.* **7**, 412 (2011).
- [15] L.Fu and C. L. Kane, *Phys. Rev. Lett.* **100**, 096407 (2008).
- [16] L. Fu and C. L. Kane, *Phys. Rev. Lett.* **102**, 216403 (2009).
- [17] A. R. Akhmerov, J. Nilsson, and C. W. J. Beenakker, *Phys. Rev. Lett.* **102**, 216404 (2009).
- [18] K. T. Law, P. A. Lee, and T. K. Ng, *Phys. Rev. Lett.* **103**, 237001 (2009).
- [19] Y. Tanaka, T. Yokoyama, and N. Nagaosa, *Phys. Rev. Lett.* **103**, 107002 (2009).
- [20] J. Linder, Y. Tanaka, T. Yokoyama, A. Sudbo, and N. Nagaosa, *Phys. Rev. Lett.* **104**, 067001 (2010).
- [21] A. Yamakage, Y. Tanaka, and N. Nagaosa, arXiv:1110.0358.
- [22] Y. S. Hor, A. J. Williams, J. G. Checkelsky, P. Roushan, J. Seo, Q. Xu, H. W. Zandbergen, A. Yazdani, N. P. Ong, and R. J. Cava, *Phys. Rev. Lett.* **104**, 057001 (2010).
- [23] L. A. Wray, S.-Y. Xu, Y. Xia, Y. S. Hor, D. Qian, A. V. Fedorov, H. Lin, A. Bansil, R. J. Cava, and M. Z. Hasan, *Nature Phys.* **6**, 855 (2010).
- [24] M. Kriener, K. Segawa, Z. Ren, S. Sasaki, and Y. Ando, *Phys. Rev. Lett.* **106**, 127004 (2011).
- [25] M. Kriener, K. Segawa, Z. Ren, S. Sasaki, S. Wada, S. Kuwabata, and Y. Ando, *Phys. Rev. B* **84**, 054513 (2011).
- [26] L. Fu and E. Berg, *Phys. Rev. Lett.* **105**, 097001 (2010).
- [27] M. Sato, *Phys. Rev. B* **79**, 214526 (2009).
- [28] M. Sato, *Phys. Rev. B* **81**, 220504(R) (2010).
- [29] T. Hsieh and L. Fu, arXiv:1109.3464.
- [30] L. Hao and T. K. Lee, *Phys. Rev. B* **83**, 134516 (2011).
- [31] S. Sasaki, M. Kriener, K. Segawa, K. Yada, Y. Tanaka, M. Sato, and Y. Ando, *Phys. Rev. Lett.* **107**, 217001 (2011).
- [32] T. Kirzhner, E. Lahoud, K. Chaska, Z. Salman, and A. Kanigel, arXiv:1111.5805.
- [33] G. Koren, T. Kirzhner, E. Lahoud, K. B. Chashka, and A. Kanigel, arXiv:1111.3445.
- [34] F. Yang, Y. Ding, F. Qu, J. Shen, J. Chen, Z. Wei, Z. Ji, G. Liu, J. Fan, C. Yang, et al., arXiv:1105.0229.
- [35] S. Kashiwaya, Y. Tanaka, M. Koyanagi, and K. Kajimura, *Phys. Rev. B* **53**, 2667 (1996).
- [36] Y. Tanaka and S. Kashiwaya, *Phys. Rev. B* **53**, 9371 (1996).
- [37] C. Honerkamp and M. Sigrist, *J. Low Temp. Phys.* **111**, 895 (1998).
- [38] M. Yamashiro, Y. Tanaka, and S. Kashiwaya, *Phys. Rev. B* **56**, 7847 (1997).
- [39] M. Matsumoto and M. Sigrist, *J. Phys. Soc. Jpn.* **68**, 994 (1999).
- [40] M. Eschrig, C. Iniotakis, and Y. Tanaka, arXiv:1001.2486.
- [41] Although a general form of  $\Delta_4$  is  $\Delta_4 = c_1\Delta\sigma_y s_x + c_2\Delta\sigma_y s_y$ , the tunneling conductance does not depend on the ratio between  $c_1$  and  $c_2$ . Thus we put  $c_1 = 1$  and  $c_2 = 0$ .
- [42] K. Yada, M. Sato, Y. Tanaka, and T. Yokoyama, *Phys. Rev. B* **83**, 064505 (2011).
- [43] M. Sato, Y. Tanaka, K. Yada, and T. Yokoyama, *Phys. Rev. B* **83**, 224511 (2011).
- [44] G. E. Blonder, M. Tinkham, and T. M. Klapwijk, *Phys. Rev. B* **25**, 4515 (1982).
- [45] S. Kashiwaya and Y. Tanaka, *Rep. Prog. Phys.* **63**, 1641 (2000).
- [46] Y. Tanaka and S. Kashiwaya, *Phys. Rev. Lett.* **74**, 3451 (1995).
- [47] L. W. Molenkamp, G. Schmidt, and G. E. W. Bauer, *Phys. Rev. B* **64**, 121202 (2001).
- [48] N. W. Ashcroft and N. D. Mermin, *Solid State Physics* (Saunders College, Philadelphia, 1976).
- [49] S. Nakosai, Y. Tanaka, and N. Nagaosa, unpublished.